Geometric field errors of Short Models for MQXF, the Nb_3Sn low-beta Quadrupole for the High Luminosity LHC

S. Izquierdo Bermudez, G. Ambrosio, H. Bajas, G. Chlachidze, J. Ferradas Troitino, P. Ferracin, L. Fiscarelli, P. Hagen, E. Holik, J. Di Marco, E. Todesco, G.L. Sabbi, G. Vallone, X. Wang

***Abstract*— In the framework of the High-Luminosity upgrade of the Large Hadron Collider, the US LARP collaboration and CERN are jointly developing a 150 mm aperture Nb_3Sn quadrupole for the LHC interaction regions. Due to the large beam size and orbit displacement in the final focusing triplet, MQXF has challenging targets for field quality at nominal operation conditions. Three short model magnets have been tested and around thirty coils have been built, allowing a first analysis of the reproducibility of the coil size and turns positioning. The impact of the coil shimming on field quality is evaluated, with special emphasis on the warm magnetic measurements and the correlation to field measurements at cold and nominal field. The variability of the field harmonics along the magnet axis is studied by means of a Monte-Carlo analysis and the effects of the corrective actions implemented to suppress the low order un-allowed multipoles are discussed.**

***Index Terms*— High Luminosity LHC, Field Quality, Magnetic Measurements, High Field Nb_3Sn Magnet.**

I. Introduction

The High Luminosity LHC upgrade aims at increasing the integrated luminosity of the LHC by a factor of 10 beyond its nominal performance expected for 2023 [1]. Part of the upgrade relies on the replacement of the single aperture quadrupoles in the interaction region (the so-called low-β or inner triplet quadrupoles). The design, referred as MQXF, foresees a 150 mm aperture quadrupole based on Nb_3Sn technology [2]. Due to the large beam size and orbit displacement in the final focusing triplet, field errors at high energy are of primary importance. The main source of these errors are inaccuracies on the conductor position in the magnet cross-section due to manufacturing tolerances on components and coil production process. A series of short models (1.2 m of magnetic lengths, called MQXFS) are currently being fabricated both by CERN and by LARP. Although the available statistics is limited, the measured values allow a first verification of the hypotheses made on field homogeneity. We pursue a detailed analysis of the room temperature magnetic measurements and the correlation with field measurements at operation conditions. Correction strategies are discussed and a summary of the faulty assembly procedures detected thought magnetic measurements is provided.

Manuscript receipt and acceptance dates will be inserted here. This work was supported by the High Luminosity LHC Project at CERN and by the DOE through the U.S. LHC Accelerator Research Program.

S. Izquierdo Bermudez, P. Ferracin, E.Todesco and G. Vallone are with CERN, 1211 Geneva, Switzerland (e-mail: susana.izquierdo.bermudez@cern.ch).

G. Ambrosio, G. Chlachidze, E.Holik and J. Di Marco are with Fermi National Accelerator Laboratory (FNAL), Batavia, IL 60510 USA.

G.L. Sabbi and X. Wang are with Lawrence Berkeley National Laboratory (LBNL), Berkley, CA 94720 USA.

Color versions of one or more of the figures in this paper are available online at http://ieeexplore.ieee.org.

Digital Object Identifier will be inserted here upon acceptance.

TABLE I
COILS AND CONDUCTOR LAYOUT ASSEMBLED IN MQXFS

	MQXFS1a/b/c	MQXF3a/b	MQXF5a
	First Generation Design	Second Generation Design	Second Generation Design
Q1	103 (RRP 132/169)	106 (RRP 132/169)	203 (PIT 192)
Q2	3 (RRP 108/127)	7 (RRP 108/127)	205 (PIT 192)
Q3	104 (RRP 132/169)	105 (RRP 132/169)	204 (PIT 192)
Q4	5 (RRP 108/127)	107 (RRP 132/169)	206 (PIT 192)

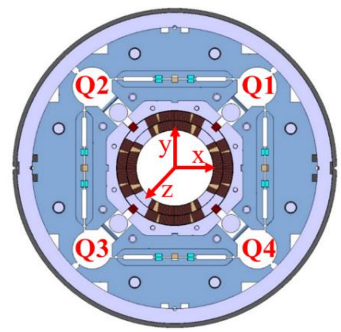

Fig. 1. MQXF magnet viewed from the lead end including coordinate axis for magnetic measurements and quadrant naming convention.

II. Magnet Assembly Parameters

The first MQXF short model (MQXFS1a/b/c) has been assembled in LBNL [3] and tested at FNAL [4]-[5], using two coils produced by LARP (coils 3 and 5) and two coils produced by CERN (coils 103 and 104). The second and the third short models (MQXFS3a/b and MQXF5a) have been tested and assembled at CERN [6]. MQXFS3 had one coil produced by LARP (coil 7) and three coils produced by CERN (coils 105-107). MQXFS5 is the first magnet assembled with coils produced in the same manufacturing line (CERN) and using a unique type of conductor. Table I summarizes the coils tested in each assembly and their relative position in the magnet (see Fig. 1).

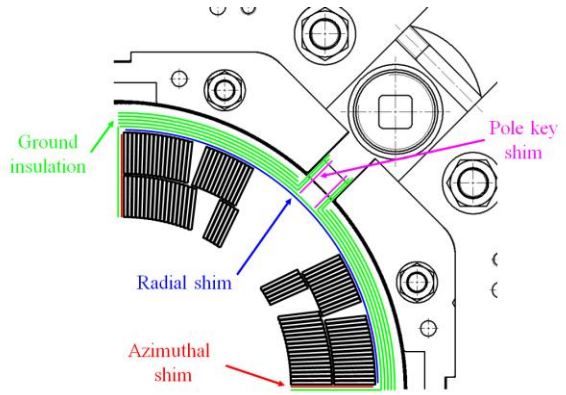

Fig. 2. MQXF cross section, showing ground insulation, radial, azimuthal and pole key shim

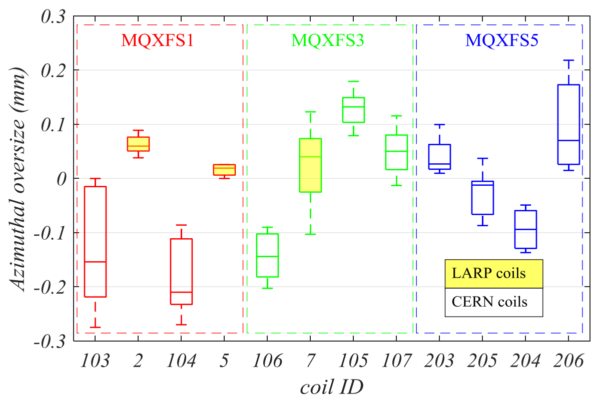

Fig. 3. Coil azimuthal size deviation with respect to nominal. Each box represents the eight cross sections measured per coil: the central line corresponds to the median, the edges of the box are the 25th and the 75th percentiles and the whiskers extend to the extreme data points.

Uniform pre-load and field homogeneity require precise coil positioning and alignment during assembly. A good matching of the outer diameter of the coils and the inner diameter of the collars is important in order to assure a proper pre-load. For field homogeneity, a good alignment of the inner diameter of the coil turns is important since the strands close to the aperture are the ones with a larger contribution to the field errors. In order to achieve this matching, the surfaces of each coil are measured by a Coordinate Measurement Machine (CMM) [7]-[8]. Each coil is measured in eight longitudinal cross sections, using the coil outer diameter and pole keyway as alignment for the CMM best fit to reproduce the functional magnet configuration. The size deviation among coils is corrected through polyimide shims aiming at having a good coil to collar matching and guarantee a uniform pre-load. Shims can be placed between the coil and the collar (radial shim), in the coil mid-plane (azimuthal shim) and in between the pole key and the collar, as shown in Fig. 2.

There are several parameters affecting the final coil size, from the specific dimensions of the reaction and impregnation tooling and tolerances to the cable expansion during heat treatment and conductor insulation [7],[9]. In average, the coil azimuthal deviation per coil side is within 0.2 mm. In some coils, azimuthal size variations up to 0.3 mm along the coil length are present. Figure 3 summarizes the azimuthal coil size deviation for the tested coils. In MQXFS1, dimensional errors were compensated using azimuthal and radial shims. In

TABLE II. AZIMUTHAL AND RADIAL SHIM DIMENSIONS TO COMPENSATE SIZE DEVIATIONS AMONG COILS.

	Quadrant	MQXFS1a/b/c	MQXF3a/b	MQXF5a
Radial shim [µm]	Nominal	0	0	0
	1	50	0	0
	2	0	0	0
	3	100	0	0
	4	0	0	0
Azimuthal shim per coil side [µm]	Nominal	0	0	0
	1	0	150	25
	2	0	50	75
	3	50	0	100
	4	0	50	0

TABLE III. AVERAGE FIELD HARMONICS IN THE STRAIGHT SECTION AFTER MAGNET LOADING AT ROOM TEMPERATURE.

	MQXFS1a		MQXFS3a		MQXFS5a	
n	b_n	a_n	b_n	a_n	b_n	a_n
3	-3.24	3.46	-1.69	-1.30	-1.30	-0.27
4	0.30	-4.18	2.13	2.75	0.55	-1.96
5	2.47	-0.55	-2.37	-1.55	0.35	-0.22
6	3.57	0.65	-1.90	0.60	-4.84	-0.08
7	0.13	0.27	0.22	-0.28	-0.61	-0.23
8	0.23	-0.25	-0.09	0.27	0.03	-0.04
9	0.15	0.31	-0.07	-0.06	0.09	-0.01
10	-0.49	0.12	0.23	-0.04	0.29	-0.08
14	-0.61	-0.03	-0.73	0.05	-0.77	-0.03

MQXFS3 and MQXFS5 the coils were shimmed only in the mid-plane since it is the best solution for field homogeneity as it will be discussed in section V. Table II summarizes the azimuthal and radial shimming layout for the three magnet assemblies. Different pole-key shimming conditions were tested. In MQXFS1, the shimming was defined to ensure contact with the collar sides at the start of the loading. In MQXFS3, a 100-µm interference was applied and in MQXFS5, a gap of 200 µm was left. Additional details are provided in [10].

III. WARM MAGNETIC MEASUREMENTS AND ANALYSIS

A. Warm magnetic measurements

The field quality in the aperture is described in a standard form of harmonics coefficients defined in a series expansion, normalized to the main field at a reference radius of 50 mm (2/3 of the aperture). Normalized harmonics are quoted in units (1 unit = 10^{-4} of the main field). The right-handed measurement coordinate system is defined with the z-axis at the centre of the magnet aperture and pointing from the return end to the lead end, as shown in Fig. 1.

For the magnets assembled and tested at CERN (MQXFS3 and MQXFS5), magnetic measurements were done using the FAME system (Fast Measurement Equipment). The horizontal rotating shaft has a radius of 43 mm and a length of 130 mm. For integral measurements, a 1.2 m shaft is used [14]. MQXFS1, assembled at LBNL and tested at FNAL, was measured using a 110 mm long rotating probe based on a printed-circuit board (PCB) technology [15]. Measurements are performed at room temperature on the coil pack assembly, on the loaded magnet and after the cold powering cycle. The measured harmonics on the loaded magnet after assembly are summarized in Table III.

TABLE IV. EXPECTED HARMONICS DUE TO ASYMMETRIC SHIMMING.

	MQXFS1a		MQXFS3a		MQXFS5a	
n	b_n	a_n	b_n	a_n	b_n	a_n
3	-1.53	1.52	0.67	-0.67	-0.68	0.00
4	0.00	-4.64	0.00	-0.72	0.00	-0.72
5	0.69	0.69	-1.33	-1.33	1.33	0.00

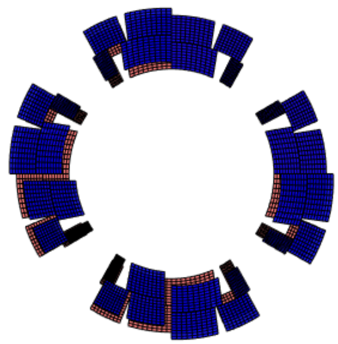

Fig. 4. Original and amplified deformed shape for MQXFS1.

B. *Systematic non-allowed field errors*

Since the coils used for the short models do not have the same azimuthal size, asymmetric shimming was required to compensate for dimensional errors and assure a uniform pre-load. The influence of the asymmetric shimming on the field harmonics was analysed imposing a deformed geometry in ROXIE [11] by means of displacements with respect to the nominal configuration. The deformed geometry is computed based on the CMM measurements of the coils and the shimming layout of the specific assembly. As an example, Fig. 4 shows the nominal and deformed shape for MQXFS1 where the differences on coil size was compensated partially on the mid-plane and partially on the coil outer radius. Expected non-allowed field errors are summarized in Table IV. When comparing to the warm magnetic measurements after loading (Table III), asymmetric shimming explains about half of the measured b_3 and a_3 in MQXFS1. Measured b_3 and a_3 are closer to expected values in MQXFS3 and MQXFS5. b_4 and a_4 are 2-3 units larger than predicted in MQXFS3 and in good agreement with expectations for the rest of the magnets. b_5 is one unit larger than predicted in all the magnets, whereas a_5 is close to the computed values.

MQXFS5, the first magnet assembled with four coils produced in the same manufacturing line, has a remarkable better field homogeneity than the previous magnets.

C. *Systematic allowed field errors*

Table V summarizes allowed multipoles measured at room temperature after loading. Measurements are compared to ROXIE computed values for different cases. The first case considers the nominal cross section assuming that the conductors are aligned to the inner diameter (ID) of the coil. The MQXF cross section was optimized assuming that the conductors are aligned to the outer diameter (OD), which corresponds to the second case. The third case computes the expected harmonics based on the actual coil geometry and shimming layout. In the fourth case, the expected coil deformation due to magnet loading is computed in ANSYS. Displacements are imported into ROXIE in order to evaluate

TABLE V. MEASURED AND PREDICTED ALLOWED MULTIPOLES AFTER LOADING (INCLUDING IRON EFFECT).

Mag.	n	*Meas.*	*ROXIE ID align*	*ROXIE OD align*	*ROXIE OD align Shims*	*ROXIE OD align Deform.*
S1a	6	3.57	-1.04	0.27	-0.02	1.17
	10	-0.49	-0.90	-0.37	-0.40	-0.34
	14	-0.61	-0.59	-0.60	-0.61	-0.60
S3a	6	-1.90	-4.83	-2.19	-1.14	-1.29
	10	0.23	-0.91	-0.11	-0.30	-0.14
	14	-0.73	-0.77	-0.79	-0.79	-0.79
S5a	6	-4.84	-4.83	-2.19	-3.32	-1.29
	10	0.29	-0.91	-0.11	-0.27	-0.14
	14	-0.77	-0.77	-0.79	-0.79	-0.79

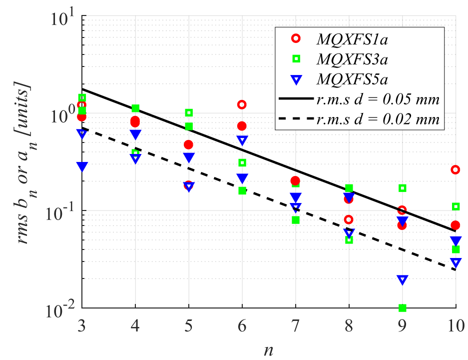

Fig. 5. R.M.S. multipole variation along magnet axis versus the order n for the assembled magnets. Filled marks correspond to skew multipoles and empty marks correspond to normal multipoles.

the impact on field quality. Measured b_{10} and b_{14} are close to expected values. In MQXFS3a and MQXFS5a, b_6 is closer to computed values when including the actual coil pack geometry and shimming layout. In MQXFS1a, measured b_6 after loading is 3.5 larger than expected.

D. *Coil waviness*

The straight part of the magnet is 0.5 m and typically around ten sections are measured with a distance in between consecutive measurements of half the mole length. The spread computed over the non-overlapping segments can provide an estimate of the precision of the coil positioning along the magnet axis [12]. Fig. 5 shows the results for MQXFS, where the spread in the position along the magnet axis is 0.04 mm for MQXFS1/S3, and 0.03 mm for MQXFS5. This spread is similar to what is obtained for the main LHC dipoles and previous Nb_3Sn magnets [13] .

E. *Variation of the geometric harmonics with magnet loading*

The alignment of the coil pack to the structure is done through the pole alignment key (see Fig. 2). MQXFS1a is the only assembly where the warm magnetic measurements before loading were done with the coil pack aligned in the magnet structure. In the rest of the assemblies, the sides of the pole key where not in contact with the collars. Fig. 7 shows that there is not a significant difference in between MQXFS1 and the rest of the magnets in terms of change on the harmonics due to magnet loading, meaning that the dominant source of field errors is the coil geometry and not its alignment on the magnet structure. The only remarkable effect of loading is 1 unit of b_4 in MQXFS3a and MQXFS5a, the assemblies where the coil pack was not aligned on the magnet structure.

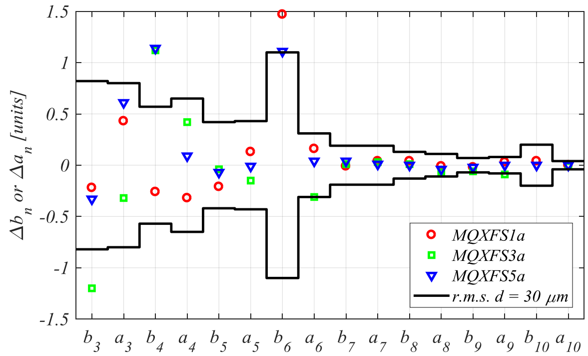

Fig. 6. Change on the harmonics from coil pack pre-assembly (MQXFS3) or coil pack including iron pads (MQXFS5) or coil pack pre-centered on the structure (MQXFS1) and to magnet loaded. Since the iron has an impact on the allowed harmonics, Δb_6 and Δb_{10} are not shown for MQXFS3.

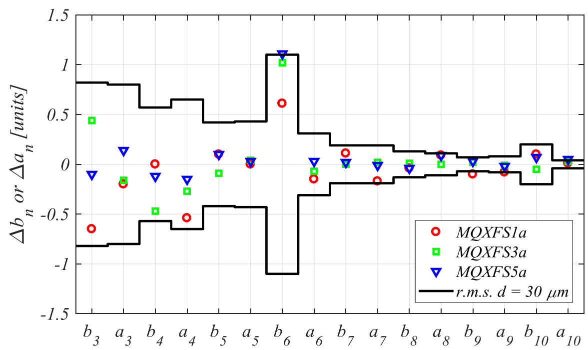

Fig. 7. Change on the harmonics from warm measurements after loading to warm measurements after magnet powering cycle.

The expected effect of loading is an increase of b_6 of 0.9 units. The measured effect in MQXFS1a is 1.5 units and 1.1 units in MQXFS5a. The value is not available for MQXF3a since the measurements before loading were performed on a temporary coil pack with no iron around the coil, which has a large contribution to the allowed harmonics. Measurements are compared to the expected harmonics due to a random displacement of the coil blocks of 0.030 mm.

F. *Variation of the geometric harmonics with cold powering*

During the cold powering test, the coils are subjected to large electromagnetic forces so it is important to evaluate if there is any permanent deformation on the coil visible on the geometric multipoles. As it can be seen in Fig 7, small variations on the harmonics are measured. The most remarkable difference is the increase of 1 unit of b_6 measured on MQXFS3 and MQXFS5.

IV. Cold Magnetic Measurements And Analysis

A. *Magnetic measurements at operation conditions*

Cold magnetic measurements at FNAL reported here are performed using a 110 mm length probe and 50.5 mm radius, installed in an anti-cryostat. The axial position of the shaft is done using a screw-driven rail with a precision of 10 µm [15]. At CERN, the shaft is composed of 5 segments, 420 mm each, and 45 mm radius. The probe shaft rotate in the helium bath and it is aligned such that the central segment covers the magnet straight section [14]. Fig. 8 shows the harmonics at

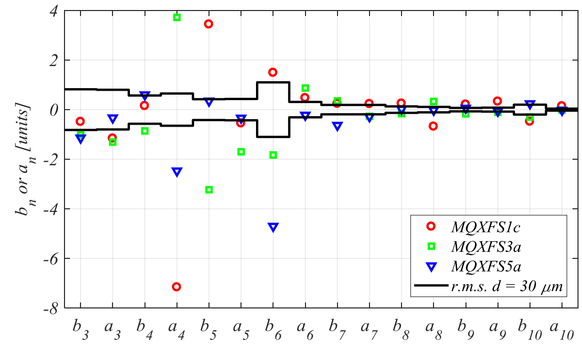

Fig. 8. Average measured harmonics in the magnet straight section at nominal field compared with target field quality (target field quality computed assuming a random displacement of the coil block of 30 µm).

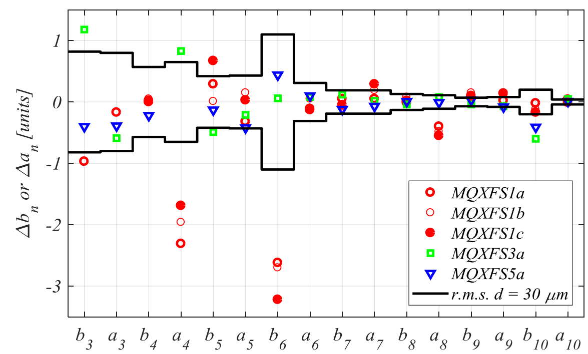

Fig. 9. Change on the harmonics from warm measurements after magnet loading to nominal operation conditions (1.9 K, 16.46 kA). Harmonics affected by magnetic shims are not shown in the plot (see section V).

nominal field averaged over the axial straight section and compares them to the target field quality based on a random error conductor position of 30 µm. a_4 and b_5 are well above targets for MQXFS1 and MQXFS3. The situation is less critical for the rest of the harmonics.

B. *Cold-warm correlation*

A high degree of cold-warm correlation is important in order to detect and compensate geometrical errors before the final assembly. Figure 9 shows the change on the harmonics from the warm measurements after loading to the magnet operating at nominal current. Apart from a_4 and b_6 in MQXFS1, the offsets are within the boundaries of a 0.030 mm random displacement of the coil blocks.

V. Corrective Actions

A. *Coil shimming*

In order to demonstrate the importance of a good alignment of the inner diameter of the coils, two coil packs assemblies were performed in MQXFS3a. For the first assembly, the coil size deviations were corrected by shimming the coil outer radius. In the second assembly, shims were placed on the mid-plane (azimuthal shimming). Table VI summarizes the measured and computed harmonics for the two cases. As expected, field errors are smaller when shimming on the mid-plane. The model predicts accurately the change on the harmonics of going from azimuthal to radial shimming (Fig 10).

TABLE VI. MEASURED AND COMPUTED HARMONICS.

	Radial Shimming				Azimuthal shimming			
	Measured		Computed		Measured		Computed	
n	b_n	a_n	b_n	a_n	b_n	a_n	b_n	a_n
3	5.81	-6.75	6.56	-6.56	-0.49	-0.98	0.67	-0.67
4	0.92	0.50	0.00	-1.81	1.01	2.33	0.00	-0.72
5	-2.48	-1.44	-1.37	-1.37	-2.33	-1.40	-1.33	-1.33

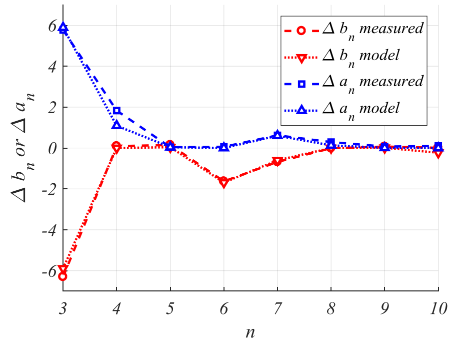

Fig. 10. Expected and measured change on the harmonics from azimuthal to radial shimming.

TABLE VII. MEASURED (COMPUTED) EFFECT OF MAGNETIC SHIMS.

	MQXFS1c		MQXFS3a		MQXFS5a	
n	Δb_n	Δa_n	Δb_n	Δa_n	Δb_n	Δa_n
3	**3.51 (4.22)**	**-3.92 (-4.24)**	1.17 (0.00)	-0.59 (0.00)	-0.40 (0.00)	-0.40 (0.00)
4	0.01 (0.00)	-1.69 (0.00)	**-2.55 (-2.88)**	0.83 (0.00)	-0.22 (0.00)	**0.71 (0.84)**

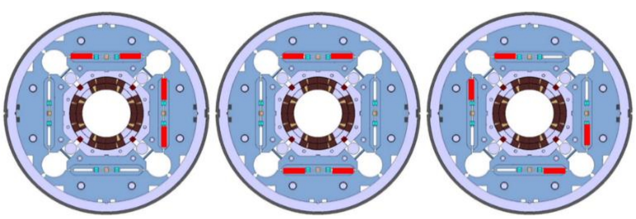

Fig. 11. Magnetic shim configuration in MQXFS1c (left), MQXF3a (middle) and MQXFS5a (right)

B. Magnetic shimming

The plan for MQXF is to correct the non-allowed harmonics through ferromagnetic shims located in the yoke, using the cavities provided to insert the pressurized bladders at assembly [16]. The technique has been tested in the short models. In MQXFS1, the shims where inserted between two thermal cycles. In MQXFS3 and MQXF5, magnetic shims were inserted during the initial assembly based on the warm magnetic measurements. Fig. 11 shows the shim configuration for the different assemblies, and Table VII compares the measured and expected variation of the multipoles. The intended correction is achieved within 10 %.

VI. FAULTY ASSEMBLY PROCEDURES

Magnetic measurements are a powerful tool for the detection of manufacturing errors and it has been intensively used for the control of magnet production. Although the available statistics in MQXF is limited to work out control limits for production, the assembly of the short models provide valuable experience for the series magnets. This section summarizes the faulty assembly procedures detected up to date through magnetic measurements.

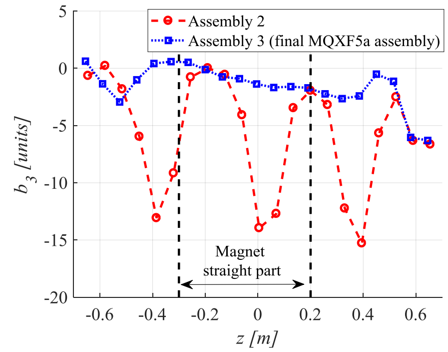

Fig. 12. Warm magnetic measurements after loading for MQXFS5 faulty assembly (Assembly 2) and the final MQXFS5a assembly (Assembly 3).

A. Pole key to collar over-shimming

A strong anomaly of 13 units of a_4 and 1 unit of a_8 was found in the coil pack assembly measurements of MQXFS5a. Inverse analysis showed that a radial misalignment of the coils of about 0.20 mm would give this effect on the multipoles. The coil pack was dismounted and revealed excessive shimming between the pole key and the collars. The coil pack was reassembled with the appropriate shims and the strong a_4 and a_8 disappeared.

B. Magnetic screws

Large variation of multipoles along the axis were found in the second coil pack assembly of MQXFS5a. The spikes were in three positions along the magnet axis and had an amplitude of 15 units in b_3/a_3 and four units in b_5/a_5. This corresponds to a random error in the position of coil blocks of about 0.15 mm. The anomalies were also visible on the transfer function. After inspection, it was found that three pre-assembly screws were not removed from the pole. These screws, made of ferromagnetic material, were the source of the large spikes. MQXFS5a was reassembled after removal of the screws and the large spikes disappeared (see Fig. 12).

C. Wrong positioning of the magnetic shims

After the cold powering test of MQXFS1a, it was decided to install magnetic shims to correct around +4 units of b_3 and –4 units of a_3. The obtained correction MQXFSb had the correct amplitude and direction in a_3, but inverted sign in b_3. The source of the error was a 180 degrees rotation on the reference frame for magnetic measurements. In addition, the shims were inserted around the coil in quadrant 4 instead of around the coil in quadrant 1. The error was corrected for MQXFS1c where the desired correction was achieved.

VII. CONCLUSION

A detailed analysis of the geometric field errors of MQXF short models has been presented. Field errors in MQXFS5, the first magnet assembled with four coils produced in the same manufacturing line, has a remarkable better field homogeneity than the previous magnets. Correction capabilities have been demonstrated, and the faulty assembly procedures identified through magnetic measurements have been discussed.

REFERENCES

[1] G. Apollinari, I. Bejar Alonso, O. Brüning, M. Lamont, and L. Rossi, "High-Luminosity Large Hadron Collider (HL-LHC): Preliminary Design Report", CERN Yellow Reports Monographs, CERN, Geneva, 2015.

[2] P. Ferracin, *et al.*, "Magnet design of the 150 mm aperture low-*β* quadrupoles for the high luminosity LHC," *IEEE Trans. Appl. Supercond.*, vol. 24, no. 3, Art. ID 4002306, 2004.

[3] H. Pan, *et al.*, "Assembly Tests of the First Nb3Sn Low-beta Quadrupole Short Model for the Hi-Lumi LHC," *IEEE Trans. Appl. Supercond*., vol. 26, no. 4, pp. 4001705, 2016.

[4] G. Chlachidze, et al., "Performance of the first short model 150 mm aperture Nb3Sn quadrupole MQXFS for the High-Luminosity LHC upgrade," IEEE Trans. Appl. Supercond., vol. 27, no. 4, pp. 1–5, 2017.

[5] G. Chlachidze et al., "Summary of test results of MQXFS1 - the first short model 150 mm aperture Nb_3Sn quadrupole for the high-luminosity LHC upgrade," *IEEE Trans. Appl. Supercond*., 2018.

[6] H. Bajas et al., "Test results of the short models MQXFS3 and MQXFS5 for the HL-LHC upgrade," *IEEE Trans. Appl. Supercond*., 2018

[7] E. F. Holik, *et al.*, "Fabrication analysis of 150-mm-Aperture Nb_3Sn Coils", *IEEE Trans. Appl. Supercond*", *IEEE Trans. Appl. Supercond*., vol 26, no. 4, 2016.

[8] J. Ferradas Troitino, *et al.*, "Applied metrology in the production of superconducting model magnets for particle accelerators", *IEEE Trans. Appl. Supercond*., 2018

[9] E. Rochepault, *et al.*, "Dimensional Changes of Nb3Sn Ruther Cables During Heat treatment" *IEEE Trans. Appl. Supercond*., vol. 26, no. 4, pp. 4802605, 2016.

[10] G. Vallone, *et al.*, Mechanical Analysis of the Short Model Magnts for the Nb_3Sn Low-β quadrupole", *IEEE Trans. Appl. Supercond*., 2018

[11] htps://cern.ch/roxie

[12] P. Ferracin, W. Scandale, E. Todesco, and R. Wolf, "Modeling of random geometric errors in superconducting magnets with applications to the CERN Large Hadron Collider", Phys. Rev. ST Accel. Beams 3, 122403, 2000.

[13] F. Borgnolutti, *et al.*, "Reproducibility of the Coil Positioning in Nb3Sn Magnet Models Through Magnetic Measurements", *IEEE Trans. Appl. Supercond*., vol. 19, no. 3, pp. 1100-1105, 2009.

[14] L. Fiscarelli, *et al.,* "Magnetic Measurements on the First CERN-built Models of the Insertion Quadrupole MQXF for HL-LHC", *IEEE Trans. Appl. Supercond.,* this conference

[15] J. DiMarco, *et al.,* "Magnetic Measurements of the Nb3SN Model Quad (MQXFS) for the High-Luminosity LHC upgrade," *IEEE Trans. Appl. Supercond.,* Vol. 27, no. 4, pp 90000105, 2016.

[16] S. Izquierdo Bermudez, *et al.,* "Second Generation Coil Design of the Nb_3Sn low-β Quadrupole for the High Luminosity LHC," *IEEE Trans. Appl. Supercond.,* vol. 26, no. 4, pp. 4001105, 2016.